BNL-220707-2020-JAAM

Not all platinum surfaces are the same: effect of the support on fundamental properties of platinum adlayer and its implications for the activity toward hydrogen evolution reaction

A. A. Koverga, J. A. Rodriguez

To be published in "Electrochimica Acta"

December 2020

Chemistry Department

Brookhaven National Laboratory

U.S. Department of Energy

USDOE Office of Science (SC), Basic Energy Sciences (BES) (SC-22)

DISCLAIMER

Not all platinum surfaces are the same: effect of the support on fundamental properties of platinum adlayer and its implications for the activity toward hydrogen evolution reaction

Andrey A. Koverga[a*], Elizabeth Flórez[a], Carlos Jimenez-Orozco[a*], José A. Rodriguez[b]

[a]Grupo de Investigación Mat&mpac, Facultad de Ciencias Básicas, Universidad de Medellín, Medellín 050026, Colombia.

[b]Chemistry Department, Brookhaven National Laboratory, Upton, NY 11973, United States

Email: akoverga@unal.edu.co (A. Koverga), cjimenez@udem.edu.co (C. Jimenez-Orozco)

Abstract

The adsorption of atomic hydrogen on a platinum monolayer supported on orthorhombic Mo_2C(100) surface has been investigated, considering different hydrogen surface coverages. Calculations have been performed using density functional theory with the Perdew-Burke-Ernzerhof exchange correlation functional and a D3 Van der Waals corrections. The theoretical insight has been gained into atomic hydrogen interaction with Pt monolayer, supported on both molybdenum and well-studied tungsten carbide, and considering hydrogen surface coverage. Fundamental properties of Pt adlayer depend on the support, affecting hydrogen evolution activity of the resulting systems. At low hydrogen coverage all systems, with the exception of Pt supported on the molybdenum-terminated Mo_2C, adsorb H comparably to a pristine Pt(111) surface and their high activity for the hydrogen evolution reaction is predicted. At higher coverages supported Pt monolayers interact with atomic hydrogen unlike the Pt(111), suggesting that the activity of the supported and unsupported platinum toward hydrogen evolution reaction have different origins. Furthermore, the position of the supported platinum monolayers on the volcano curve is a function of the surface coverage, more so than for extended metal surfaces. Therefore, hydrogen surface coverage is a key variable to understand the catalytic potential, approaching towards an improved model for screening of electrocatalytic systems.

Keywords: DFT, electrocatalysis, HER, Pt, supported monolayer, TMC.

1 Introduction

Hydrogen is considered as a sustainable and environmentally friendly alternative to carbon-based energy carriers. Its potential use, however, only has a good perspective if hydrogen production can be carried out in a low-cost and “green” fashion. These requirements are fulfilled *via* the electrocatalytic hydrogen evolution reaction (HER), a highly attractive process [1,2] which can be written as

$$H_2 \rightarrow 2H^+ + 2e^- \text{ (acidic media)} \qquad (1)$$

or

$$H_2 + 2OH^- \rightarrow 2H_2O + 2e^- \text{ (alkaline media)} \quad (2)$$

The quantification of the catalytic activity of a given material towards the HER can be done either by measuring its exchange current density by using the Tafel approach from polarization curves [3,5], by measuring the current density at a fixed overpotential, or by measuring the overpotential at a fixed current density. All these methods strongly rely on the proper evaluation of the electrochemically active surface area, which may be one of the most challenging issues in electrochemistry. Different materials show better or worse exchange current density at the same overpotential, which leads to improved or decreased electrocatalytic activity towards HER, respectively. Nowadays, platinum is the best known catalyst for the HER [3-6].

Unfortunately, high market prices and scarcity of this precious metal in the Earth crust limit production of devices requiring large Pt loadings for massive production of hydrogen using the HER [7,8]. Therefore, to make this method viable it is important to find an alternative to Pt-based materials, which could allow a significant decrease in the usage of Pt (or avoiding its use), together with a minimal loss in electrocatalytic activity.

In practical terms, deploying Pt nanoparticles onto a low-cost support of choice is the current methodology for producing these materials [9,10]. However, this method does not utilize the core of the supported nanoparticles, which is a serious disadvantage for a cost optimization. To overcome this drawback and even further minimize the Pt loading, a supported Pt monolayer can be used as reported by Esposito *et al.* [9] They demonstrated that transition metal carbides (TMCs) have remarkable potential as supports, due to the closeness of their catalytic and electronic properties to those of Pt-group materials [11]. Among TMC, tungsten (WC) and molybdenum carbide (Mo_2C) have an additional advantage: their good stability in electrochemical media at typical HER conditions [12,13].

Experimental works already conducted for a Pt monolayer (ML) supported on WC and Mo_2C, evidence that TMCs are able to effectively replace the bulk of precious metal catalyst with a remarkable HER activity, comparable to that of pure platinum [14,15]. It is important to mention here that Esposito *et al.* clearly demonstrated that composite systems, comprised of a Pt ML and tungsten carbide as support, show a correlation between HER activity and hydrogen binding energy [10], similarly to pristine metallic catalysts. Therefore, the HER activity of Pt/TMC catalysts can be initially estimated by analyzing H adsorption on the surfaces of interest.

A number of theoretical studies examining the Pt/WC system were aimed at gaining an insight into Pt–WC interaction and to explain why this system displays an activity comparable to pure Pt [16-18]. These studies clearly demonstrated that the electronic properties of Pt supported on WC and, consequentially, its activity towards HER, experience an impact from the support and are mainly defined by ligand (*d*-band stabilizing) and strain (*d*-band destabilizing) effects. Theoretically predicted exchange current density values for Pt/WC were found to be in a good agreement with the experimental data, as reported by Esposito and Chen [14].

Notably, there is a surprising lack of theoretical works exploring the Pt/Mo_2C system in terms of its potential catalytic activity for the HER. Also, not much has been done for hydrogen adsorption on Pt/TMCs surfaces at varying H coverage. Even though the Pt/WC catalyst already has been studied extensively, a systematic analysis of different configurations for this system is useful to optimize its performance. At the same time examining the changes in the electronic structure of Pt ML supported on Mo_2C provides a novel information on this system in the scope of its HER activity, especially because WC and Mo_2C have different crystal lattices and do interact with Pt in a different way.

Here, low-coverage hydrogen adsorption was considered on Pt/α-WC and Pt/β-Mo_2C surfaces with the aim to estimate changes in H–Pt interactions caused by the presence of the TMC supports. The α-WC(0001) [19] and β-Mo_2C(100)20 (also known as β-Mo_2C(001) for some authors [21-23]) surfaces are used, since they have been reported in several experimental studies [9,15]. Furthermore, adsorption energies for atomic H on low-index surfaces of metals, used to build the volcano curve in the study of Nørskov *et al.* [3], were recalculated using the same parameters as for Pt/TMC to obtain a volcano curve with an improved accuracy and to place the studied systems on the curve. Finally, the effect of growing H coverage on the volcano curve and on the stability of atomic H on the Pt/TMC surfaces is reported, together with changes in the positions of these systems on the volcano curves, in order to estimate whether the inclusion of the coverage effect influences the predictive ability of this method.

2 Computational details

Periodic density functional calculations were performed using the Vienna *ab initio* simulation package (VASP) [24-27] within the generalized gradient approximation, utilizing Perdew, Burke and Ernezerhof for the exchange-correlation energy functional [28], together with the Projector Augmented Wave core potentials [29] as implemented by Kresse and Joubert [30]. To improve the description of the long-range correlation effects, the van der Waals (vdW) correction proposed by Grimme [31], namely its D3 scheme [32], was used.

Dipole corrections were also applied throughout the calculations to avoid dipole coupling between repeating images of the unit cell, in the direction perpendicular to the surface. The kinetic energy cut-off of 415 eV for the plane wave basis set was selected, which is enough to obtain reproducible and reliable results on systems with carbides [21,22]. Integration of the reciprocal space for all surfaces was carried out using 3 × 3 × 1 grids of special ***k***-points within Monkhorst-Pack scheme [33] for the geometry optimization procedures; while 11 × 11 × 1 grid was used for the Density of States calculations. A 1 × 1 × 1 mesh was used to obtain total energy of atomic and molecular hydrogen in vacuum, The Fermi level was smeared using the Methfessel-Paxton approach [34] with a Gaussian width of smearing of 0.2 eV.

When dealing with metal carbides, the notation of the crystal systems could be confusing since there is not a standard one. In this work we follow the nomenclature previously reported by Kurlov and Gusev for WC [19], while for Mo_2C, we use the nomenclature defined by the Joint Committee on Powder Diffraction Standards (JCPDS) data files [21]. Therefore, in this work, we refer to Pt/α-WC and Pt/β-Mo_2C. The hexagonal phase of tungsten carbide (α-WC) and orthorhombic molybdenum carbide (β-Mo_2C) were considered in this study as the supports for Pt, specifically the α-WC(0001) and Mo_2C(100) surfaces, with their corresponding polar metal- and carbon-terminations.

Pristine C- and M-terminated surfaces, in this work denoted as C-WC, C-Mo_2C, W-WC and Mo-Mo_2C, were represented by (4×4) supercells, each of them comprised of two metal and two carbon alternating atomic layers. A vacuum region on 13Å was added to each cell to prevent interactions between repeating images of the slab in *z* direction. To assure that the selected number of atomic layers in each supercell was sufficient to obtain correct energy values, calculations for a single Pt atom adsorption on the C-WC, C-Mo_2C, W-WC and Mo-Mo_2C were repeated using thicker slabs comprising five layers. The obtained adsorption energies on four-layer and five-layer slabs were in general very close (-6.17 eV versus -6.14 eV for C-Mo_2C; -6.68 eV versus -6.56 eV for Mo-Mo_2C; -6.02 eV versus -5.94 eV for C-WC; and -6.50 versus -6.39 eV for W-WC), with differences smaller than 0.15 eV, confirming the adequacy of the selected model.

Supported Pt monolayer was modeled by completely covering the transition metal carbide (TMC) support with platinum atoms (preventing any interaction of the TMC with adsorbed hydrogen); hence, in total 16 Pt atoms were present in each Pt/TMC system. Structure optimization calculations have been carried out using a (1+2+2) approach, *i.e.* for Pt supported on the TMC terminations 2 out of 4 total atom layers of the support were allowed to relax simultaneously (topmost layers), while 2 remaining (bottom) layers were frozen to represent bulk of the support. The adsorbates were allowed to relax in all three directions together with the supported Pt monolayer. Such an approach to the modeling of the TMC and M/TMC surfaces have delivered in the past reliable data on surface–adsorbate interactions [22,23,35,36].

The platinum (111) surface has been represented in a similar manner, using a (4×4) supercell with (2+2) approach. All the model setup parameters were kept identical, to assure the consistency of the obtained results. For other metals, used to obtain the volcano curve , the adsorption of atomic hydrogen has been considered under the same model setup on the corresponding (111) surfaces for Au, Ag, Cu, Ir, Ni, Pd and Rh, (001) – for Co and (110) – for Mo, Nb and W [3].

The hydrogen coverage for systems with surface platinum atoms, Θ_H, can be defined as a ratio between total number of hydrogens on a studied surface and the number of exposed Pt atoms. Thus, for a system with 16 H atoms and 16 Pt surface atoms Θ_H is 1 ML; for a single atomic hydrogen adsorbing on the same surface the coverage would be 1/16 ML. For each Pt/TMC and for Pt(111) surfaces atomic hydrogen adsorption has been

considered at all hydrogen coverages in the range from 1/16 to 1 ML, while for metals, used to build the volcano curve, H adsorption at Θ_H = 1/16, 1/4, 1/2 and 1 ML was analyzed.

Pt bulk cohesion energy was estimated from the expression

$$E_{coh} = \frac{E_{Pt_n} - nE_{Pt}}{n} \qquad (3)$$

where E_{Pt_n} and E_{Pt} are total energies of a cell consisting of n Pt atoms in bulk geometry and isolated Pt atom, respectively.

The adsorption energy (E_{ads}) for Pt monolayer was calculated as proposed by Vasić *et al.* [17] (Integral Binding Energy, in terminology of the authors):

$$E_{Ads} = \frac{E_{Pt+TMC} - 16 \times E_{Pt_g} - E_{TMC}}{16} \quad (4)$$

where E_{Pt+TMC} is the total energy of system with Pt monolayer placed on the TMC surface, E_{Pt_g} – energy of the isolated Pt atom in the vacuum and E_{TMC} – total energy of pristine TMC surface.

Adhesion energy (E_{Adh}) of the Pt monolayer on TMC surfaces can be calculated using E_{ads}:

$$E_{Adh} = E_{Ads} - \Delta E_{Surf} - \Delta E_{Pt} \qquad (5)$$

ΔE_{Surf} here is the difference between the energy of the surface with the geometry adopted upon Pt monolayer adsorption and of the isolated surface with relaxed geometry. ΔE_{Pt} is the difference between the energy of isolated monolayer structure frozen in the geometry that it adopts upon adsorption on TMC surface and the energy of the Pt structure, consisted of 16 atoms after relaxation in the gas phase. The degree of strain (S) was defined as proposed by Posada-Pérez *et al.* in [37] and calculated as

$$S = \frac{d_{Pt\text{-}Pt(ML)} - d_{Pt\text{-}Pt(Bulk)}}{d_{Pt\text{-}Pt(Bulk)}} \times 100\% \quad (6)$$

$d_{Pt–Pt(ML)}$ and $d_{Pt–Pt(Bulk)}$ are the average Pt–Pt distance in the monolayer and in bulk respectively. From this formalism, positive values would indicate expansion while negative contraction of the structure compared to the bulk geometry.

Adsorption energies for atomic hydrogen on Pt/TMC surfaces can be obtained from expression

$$E_{Ads,H} = E_{Surf+H} - E_{Surf} - \frac{1}{2} E_{H_2,g} \quad (7)$$

E_{Surf+H}, E_{Surf} and $E_{H2,g}$ are energies of the system with adsorbate on the surface, of the pristine surface and of the hydrogen molecule in gas phase, respectively.

Bader charge analysis [38] has been performed on bare Pt/TMC systems and surfaces with atomic hydrogen as implemented in VASP by Henkelman, Arnaldsson and Hannes [39]. From data on the charge distribution, charge density difference (CDD) can be calculated as

$$\Delta\rho=\rho_{TMC+Pt+Ads}-\rho_{TMC+Pt}-\rho_{Ads} \quad (8)$$

$\rho_{TMC+Pt+Ads}$ is charge distribution in the system with an adsorbate on a Pt/TMC surface, ρ_{TMC+Pt} and ρ_{Ads} are charge distributions in the systems consisted of TMC-supported Pt monolayer and of an adsorbate in the gas phase, respectively. It is important to note here that CDD can only be correctly calculated under the strict condition that ρ_{TMC+Pt} and ρ_{Ads} components of the studied systems are obtained using exactly the same geometries as they have in the composite system [40]. The CDD can be visualized by additional software tools like VESTA [41] or VMD [42].

On the TMC surfaces, several adsorption sites for Pt, described for the terminations of α-WC(0001) [35] and Mo_2C(100) [22,43] have been considered (see Figure S1). After obtaining stable geometries of Pt/TMC systems, sites available for H adsorption on Pt/β-Mo_2C and Pt/α-WC these surfaces were selected, as indicated in the Figures 1 and S2, respectively. The study for hydrogen adsorption to place Pt/TMC on the volcano curve of the HER activity has been performed by placing one H atom on the surface; therefore the initial coverage, Θ_H was 1/16 ML on Pt/TMC surfaces and on the surfaces of the metals, used to build the volcano curve.

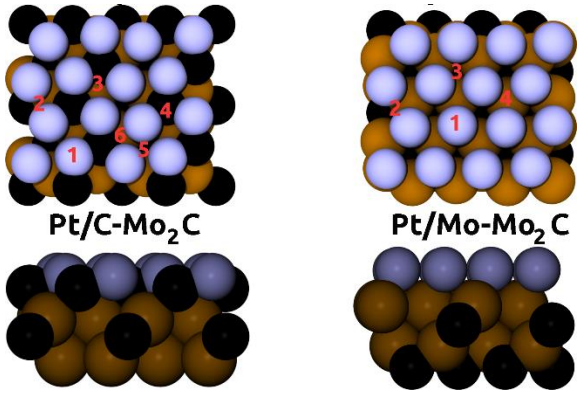

Figure 1. Pt ML structures supported on the terminations of Mo_2C(100) surface: upper panel—top view, lower panel—side view. Black, ocher, and pale blue spheres represent carbon, molybdenum and platinum atoms, respectively. Available adsorption sites on Pt/C-Mo_2C are: 1–top, 2 and 3–distinct bridge sites, 4–C*hcp*, 5–E*hcp*, 6–Mo*hcp*; on Pt/Mo-Mo_2C: 1–top, 2–bridge, 3–E*hcp*, 4–Mo*hcp*

For the detailed analysis of H-Pt interaction in Pt/TMC systems and to investigate the changes in atomic hydrogen adsorption energies on extended metal surfaces and Pt/TMC surfaces with hydrogen coverage a stepwise adsorption reported in other works [44,45] was used:

$$E_{ads,nH} = E_{Surf+nH} - E_{Surf+(n-1)H} - \frac{1}{2} E_{H_{2,g}} \quad (9).$$

Here $E_{Surf+nH}$ is the total energy of a system with *n* H atoms adsorbed on the surface; $E_{Surf+(n-1)H}$ – corresponds to the total energy of a system with *(n-1)* H atoms on the same surface, and $E_{H2,g}$ – is the energy of a H_2 molecule in gas phase.

3 Results and discussion

3.1 Interaction of Pt with TMCs

Adsorption of a single Pt atom on both terminations of β-Mo_2C(100) was studied first to define the preferable adsorption locations for platinum and then reach the monolayer coverage on this support. Results on Pt interaction with α-WC(0001) and formation of the monolayer were compared to previously published data [18,46] to confirm the reliability of the selected model parameters used in this work.

On polar terminations of β-Mo_2C various top, bridge and hollow sites were analyzed in agreement with the work of Posada-Perez *et al.* [22], while for tungsten carbide surfaces, top, bridge and *hcp* sites were considered, as described in previous work [35] (Figure S1). After the relaxation, the Pt atom was found to settle on three atoms-coordinated sites of β-Mo_2C support with no atom directly underneath it, regardless the termination of the surface (E*hcp* site). It is not possible, unfortunately, to directly compare these preferable sites with previously published data, since Pt interaction with molybdenum carbide is not as well studied theoretically as with α-WC(0001). Therefore, to the best of our knowledge, the current study is the first one to contribute to the understanding of Pt on β-Mo_2C(100). However, on α-WC(0001), according to our calculations, Pt preferably adsorbs on C*hcp* sites of the W-WC (E_{ads} = -6.50 eV) and on E*hcp* sites of C-WC (E_{ads} = -6.02 eV) surfaces. These preferred adsorption sites are in good agreement with previously published studies [16,17,47]. Furthermore, calculated adsorption energies (see Table S1) are quite close to those reported by Vasić *et al.* [17], pointing to the reliability of the selected model setup.

Sixteen Pt atoms were added to the corresponding most stable sites of the surfaces, to build a platinum monolayer coverage on each TMC, and the systems were allowed to relax. Obtained structures on the terminations of β-Mo_2C are shown in Figure 1, while the Pt/α-WC geometries can be seen in Figure S2. Selected properties, such as monolayer adsorption and adhesion energies, the degree of strain of the Pt structures, and net charge in the platinum monolayer can be seen in Table 1.

Table 1: Adsorption energy per atom, (E_{ads}) and adsorption energy of the last Pt atom in the monolayer ($E^{ML}_{ads,Pt}$), average normal Pt–TMC distance (d(Pt-TMC)), adhesion energy (E_{adh}), degree of strain (S) and average net charge per Pt atom (Q) for the optimized Pt structures on β-Mo_2C(100) and α-WC(0001) terminations.

TMC termination	E_{ads} (eV)	$E^{ML}_{ads,Pt}$ (eV)	d(Pt-TMC) (Å)	E_{adh} (eV)	S[a] %	Q[b] (*e*)
C-Mo_2C(001)	-6.83	-7.22	0.62	-8.09	+10.6	-0.13
Mo-Mo_2C(001)	-7.12	-7.56	2.03	-7.70	+8.9	-0.39
C-WC(0001)	-6.53	-6.16	1.21	-7.31	+4.3	+0.19
W-WC(0001)	-7.50	-7.86	2.09	-7.50	+4.3	-0.43

[a] Positive values correspond to an expansion process.

[b] Negative and positive values correspond to charge gain and loss, respectively.

Calculated E_{ads} values for a Pt monolayer on the α-WC support are in good agreement with the values, reported for these systems [18]. From the data in Table 1 it can be seen that for both TMC supports their termination has an impact on the Pt–TMC interaction: the stability of the monolayer is higher on the metal terminations of the TMC in respect to C-Mo_2C and C-WC. Additionally, location of Pt on the C-Mo_2C surface leads to more stable structures as compared to C-WC. To verify whether the monolayers of Pt are indeed formed on α-WC(0001) and β-Mo_2C(100) surfaces, the binding energies of Pt atoms were compared with the bulk cohesion energy of Pt (-5.58 eV, which is close to the typical value obtained using PBE functional [48]).

A metal interacting with the support can either form a bulk-like particle or a thin film, depending on whether the binding energy of this metal is larger or smaller than its cohesion energy [49]. Therefore, if the binding energy of the Pt atoms on the TMC surface is smaller than the E_{coh}, Pt atoms would preferably bind one to another and form large bulk-like nanoparticles. In the opposite case, when the binding energy is larger than the E_{coh}, Pt will cover the support and form a continuous film. The Pt binding energy in all cases is significantly larger than -5.58 eV, therefore indicating that the Pt monolayer should form and be stable on α-WC(0001) and β-Mo_2C(100) surfaces. These values, combined with a simple analysis, available in Section S1 of the Supplemental Information, also evidence that the Pt/TMC systems are expected to show a good stability in the range of potentials where the HER takes place.

An analysis of the adhesion energy showed that for Mo-Mo_2C the difference between the average adsorption energy of Pt in the monolayer and E_{adh} is ~ 0.6 eV, suggesting that the adsorption of the Pt monolayer on this

support takes places with a significant deformation of both the monolayer and the surface. An even bigger difference between the values of E_{ads} and E_{adh} in the case of C-Mo_2C evidences a larger simultaneous deformation of the TMC surface and Pt monolayer upon their interaction.

For the W-terminated α-WC support, the calculated adhesion energy does not differ from the adsorption energy, indicating that the surface and monolayer deformations are not dominant upon Pt ML adsorption; while on C-WC, similarly to C-Mo_2C, the monolayer–support interaction leads to their deformation as compared to the geometry of the surfaces before locating the Pt.

After a detailed analysis for the geometry of Pt/TMC systems, it becomes evident that on both C-Mo_2C and C-WC supports, the average Pt-TMC normal distance is quite small (1.21 Å and 0.62 Å for α-WC and β-Mo_2C, respectively); while on M-terminated supports this distance is close to 2 Å. Similar tendencies have been observed for Cu/WC system, in which Cu–WC distance was significantly smaller on W-WC support, as compared to C-WC [36]. This fact may impact the activity of the Pt/TMC systems for HER since it may result in Pt-mediated interaction between the TMC and an adsorbed hydrogen, leading to alterations in its stability on the composite surface.

In all the Pt/TMC systems, the Pt–Pt distances are larger than in bulk Pt, as suggested by the positive strain degrees (Table 1) and originates from the distances between the preferable adsorption sites for Pt on all TMC surfaces, that are larger than the Pt–Pt distance in bulk platinum. The organization of the Pt atoms on Mo-Mo_2C resembles a slightly deformed hexagonal structure with the internal Pt–Pt–Pt angles varying from 116^o to 123^o (see Figure S3). In the same figure, it can be seen that the interactions of Pt with the exposed carbon atoms of Pt/C-Mo_2C, leads to even more irregular monolayer structure in this system, as the significant departure of the internal angles from 120^o indicates. This geometry is the result of the structure of the upper layer of this termination: unlike in C-WC system, where there are as many C atoms as W in varying atomic layers, on C-Mo_2C carbon atoms do not cover completely the underlying Mo atoms, making them available for the interaction with platinum. Because of this, Pt atoms supported on C-Mo_2C form a layer that interacts with the molybdenum atoms in the sublayer and incorporates the exposed C atoms into its structure, leading to the significant departure from an hexagonal organization. This fact also explains the smaller difference between adsorption energies for Pt on the terminations of β-Mo_2C(100), than those observed for the α-WC(0001) support.

On the α-WC support, regardless of the termination, Pt monolayer maintains a hexagonal structure with all the internal angles of 120° because of the hexagonal crystalline structure of the support itself. Similar organization of Pt on C-WC support has been reported by Vasić *et al.* [17] and on W-WC support by Anićievič *et al.* [18]

On Mo-Mo_2C, a charge transfer is observed from the support to the Pt monolayer, while on C-Mo_2C, direction of the charge transfer remains the same (Figure S4), although trice as small in its magnitude. This observation can be explained by the proximity of the molybdenum atoms to the monolayer, as described above, because of which each Pt atom is able to acquire the charge from the molybdenum atoms that are in contact with it. The total amount of charge transferred to the atoms of the monolayer is smaller than on Mo-Mo_2C, due to the presence of C atoms of the support in contact with Pt atoms, drawing an excess of charge from them.

The average charge on atoms of β-Mo_2C that are in contact with Pt atoms of the monolayer, compared to the average charge of the same atoms without the monolayer is listed in Table S2. It can be seen that in the C-Mo_2C system the presence of Pt causes a decrease of an average charge on the C atoms from -0.71 *e* to -0.66 *e*; molybdenum that is in the vicinity of Pt, in its turn, becomes more positive with respect to its average charge in the pristine C-Mo_2C surface (+0.81 vs. +0.71 *e*), confirming a significant Pt—Mo interaction in this system. On Mo-Mo_2C, carbon atoms retain their charge of -1.34 eV with and without Pt, while a significant charge loss is observed for Mo atoms (from +0.32 *e* in the pristine Mo-Mo_2C to +0.73 *e*), suggesting that in Mo-Mo_2C system Pt mainly interacts with molybdenum atoms.

On a α-WC surface, a significant difference in the charge distribution between Pt and the support has been observed, depending on its termination (Figure S4). On C-WC, there is a charge transfer from the monolayer to the support, and Pt atoms on the surface acquire a net positive charge. At the same time, on W-WC Pt atoms are reduced, due to a charge transfer from the tungsten atoms of the support to the Pt atoms (see Table 1). Similarly, Table S2 evidences that atoms of the support in direct contact with Pt experience significant changes in their average charge. On C-WC exposed carbon atoms gain additional 0.25 *e* from the Pt monolayer, while on W-WC tungsten atoms lose 0.45 *e* due to the presence of platinum on the support. These observations complement well the analysis of charges of Pt atoms in the monolayer.

In W-WC this phenomenon takes place because in surface, the charge transfer takes place from metal to carbon, in the direction from the slab exposed to vacuum into the bulk of the system [36]. The opposite behavior has been reported for β-Mo_2C(100) bare system [20]; therefore, the electron density in bare α-WC and β-Mo_2C(100) systems is also different. The dipole moment is aligned along the positive *z* direction and when the Pt monolayer is placed on a surface with exposed Mo or W atoms, a charge transfer in the *z* direction to Pt takes place to compensate the surface dipole. A particular process occurs in Pt/C-WC system where the supported monolayer is oxidized, while on C-Mo_2C Pt remains reduced because of the higher Mo:C ratio than in C-WC, which somewhat compensates charge transfer from/to Pt and the support. Similar charge transfer from/to the support and the monolayer as a function of the termination of the support has been also reported for Cu adsorbed on molybdenum [37] and tungsten carbides [36]. This suggests that similarly to copper, the chemical properties of Pt supported on a TMC would reflect an impact of the support's termination.

The effect of the support and its termination can be further estimated by analyzing the electron localization function (ELF) plots of the systems (Figure S5). For Pt/α-WC system a higher concentration of electrons is observed around a Pt monolayer on Pt/W-WC than on Pt/C-WC. The ELF plots for Pt/β-Mo_2C evidence a significantly smaller difference between electron localization around the monolayer on C- and Mo-terminations, which is explained by the fact that regardless of the termination, Pt is able to interact with molybdenum atoms of the support, as described above, confirming the results on average charge of Pt atoms (Table 1) and atoms of the TMC supports in contact with the monolayer (Table S2).

To get a better understanding of the effect of support on Pt monolayer electronic properties, an analysis of the normalized *d*-Projected Density of States (PDOS) has been conducted. A shift in the Pt density of states away from the Fermi level is observed for platinum atoms in the Pt/TMC systems (Figure 2) regardless of the support and its termination. To quantify this impact, an analysis of the *d*-band center position has been performed to evaluate this shift, since the *d*-band center of surface atoms is an important property defining surface adsorption capability [50,51].

The *d*-band model [50] states that a positive shift of the d-band center, or upshift, leads to a lower occupation of anti-bonding states in the adsorbate–surface interaction, stabilizing the adsorbate; a negative shift, or downshift, weakens the adsorbate–surface interaction. Therefore, by analyzing changes in the *d*-band center position it is possible to predict changes to the catalytic properties of the materials relative to some selected reference system.

Using this correlation, a downshift of the *d*-band center would weaken the adsorption of the HER intermediates and, consequently, reduce the catalytic activity of the Pt/TMC systems for this reaction. The *d*-band centers for the supported Pt monolayers were calculated for all the studied systems and the values are given in Figure 2. Downward shifts are observed for all the Pt/TMC systems, with respect to the *d*-band center of Pt(111), and, therefore, it is expected that on these surfaces, adsorption of HER intermediates would be less stable than on clean Pt(111). These results are reliable since for a Pt monolayer on the α-WC support the *d*-band center downshift has been reported already in [17] and [18], although its values were found to be slightly higher than those in the present work (see Table S3). This discrepancy can be attributed to a slightly more positive value for the Pt(111) *d*-band center reported in the mentioned studies (-2.26 eV) compared to the value of -2.58 eV used here, or compared to those reported in other works (-2.42 [52], -2.72 [53] or -2.62 eV [54]), where our value is within the range of reported data.

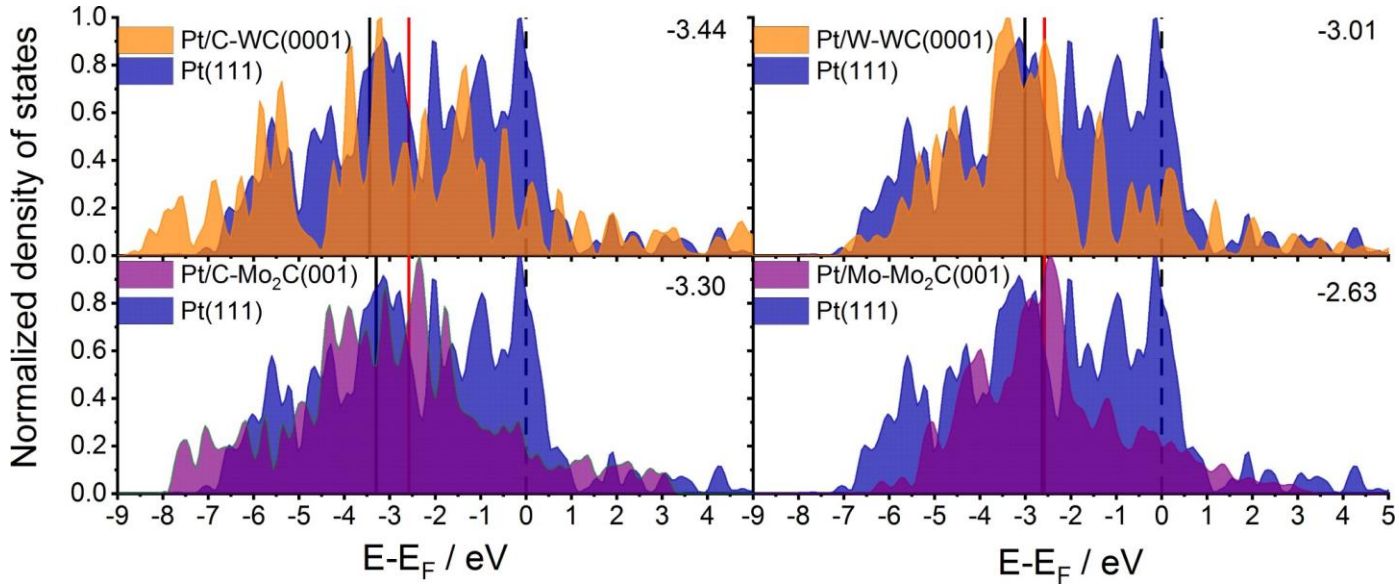

Figure 2. Normalized d-projected densities of states (PDOS) of Pt monolayers supported on M- and C-terminated α-WC(0001) and β-Mo_2C(100). For each system, the Fermi level (dashed line), position of the *d*-band center (solid black line) and its value (upper right corner of each panel) and Pt(111) *d*-band center at -2.58 eV (solid red line) are indicated.

Based only on the *d*-band center position, a lower activity of Pt/TMC systems towards HER than of Pt(111) would be expected. However, other factors that influence stability of the intermediates must be considered to be able to draw a general conclusion about the performance of Pt/TMC systems as a catalyst for HER. These factors include but are not limited to the degree of strain, which reduces the overall coordination of supported metal atoms; plus the distance between the TMC support and the supported Pt that may affect the charge transfer between the adsorbate and supported metal (monolayer) on the TMC [36] .

3.2 Atomic H adsorption on Pt/TMC surfaces

Generally, a fundamental understanding of how catalytic activity is tied to the structure and physical properties of materials is critical to choose/identify an effective activity descriptor and develop efficient computational models for an accurate description of catalysts. In case of the HER, variations in the *d*-band center [50] and the work function [5] from one material to another would also change the interaction of reactants and intermediate species with the surface. In acidic media, the reacting species is expected to be H^+ and therefore, hydrogen binding energy is commonly used for a preliminary estimation of catalytic activity as well [3,55]. Similarly, thought in alkaline media water is the expected reacting species, it must be mentioned that atomic hydrogen binding energy also appears to correlate well with HER activity [56]. Therefore, in a first approximation to the problem, a systematic study of H adsorption on Pt/TMC surfaces is required to get a conclusive understanding of the impact of the support on the overall catalytic performance of these systems.

Analyzing adsorption energies for H on Pt available in the literature, it is important to keep in mind that E_{ads} values depend on the parameters of the selected model, such as H coverage, choice of the pseudopotential, slab thickness among others. Because of this, reported values for $E_{ads,H}$ on Pt(111) surface vary from -0.33 eV [3] and -0.45 [17,18,46] to -0.52 eV [57]. Our result of -0.59 eV is somewhat higher than these values, which can be attributed to factors such as lower Θ_H in the present study, usage of a D3 Van der Waals corrections and differences in the software packages used in the present work and in the mentioned studies.

Another way to verify the model is using the calculated adsorption energies of atomic H on the surface terminations of the TMC. Although adsorption of atomic hydrogen on TMCs is rather a complex process, which causes surface reconstruction in some carbides [58,59], these effects have been not reported so far to take place for WC and Mo_2C. On the C-termination of pristine tungsten carbide, atomic H adsorbs atop of a surface C atom while on W-termination the preferable site is E*hcp*. Adsorption energy values calculated in this work were -1.59 and -1.19 eV for C- and W-terminated α-WC(0001) surfaces, respectively, and are in good agreement with -1.55 eV [60] and -0.99 [10,61] for the same terminations. For the adsorption on β-Mo_2C(100), the obtained energies of -0.89 eV (C-Mo_2C) and -1.04 eV (Mo-Mo_2C) are also close to those reported previously for these surfaces [43].

Stable geometries for H on Pt/β-Mo_2C and Pt/α-WC surfaces obtained after the relaxation are shown in Figures 3 and S6, respectively and Table 2 summarizes selected adsorption characteristics, together with those on Pt(111) for comparison purposes. It can be seen that in most of the cases adsorption of H atom does not cause any significant changes in the monolayer's geometry, with the exception of Pt/C-Mo_2C system. There the carbon atom of the TMC support is able to interact with atomic hydrogen directly, due to very small C–Pt distance in this system (see Table 1) and form a stable C–H covalent bond, yanking C atom of the TMC from the surface to the distance 1.26 Å (Figure 3). Another interesting feature associated with the β-Mo_2C support is that in Pt/Mo-Mo_2C system atomic H, adsorbing on Mo *hcp* site comes very close to the support, placing itself inside of the Pt monolayer and causing an increase in Pt–Pt distances in its vicinity from an average value of 2.95 Å to 3.42 Å. This process is quite similar to hydrogen migration from metal catalyst particle onto the catalyst support, reported for platinum, supported on alumina [62], silica [63], iron oxide [64] and molybdenum oxide [65] among others and to our knowledge has not been reported for TMC-supported platinum systems. An increase in the Pt–Pt distances for platinum atoms, close to the hydrogen atom, has been observed also for other adsorption sites on Pt/Mo-Mo_2C, although not exceeding 3.25 Å. The H adsorption on E*chp* site of Pt(111) does not alter Pt–Pt distances, suggesting that on β-Mo_2C(100), Pt ML atoms can move easier than in Pt(111).

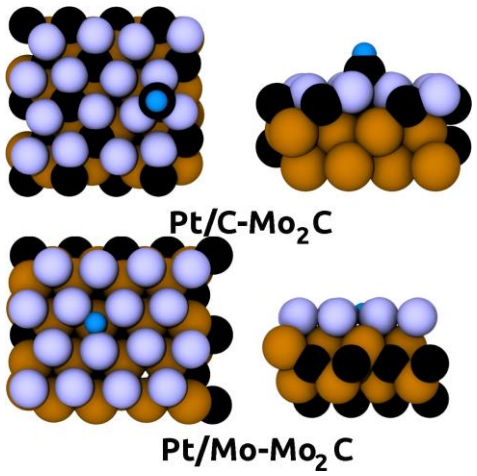

Figure 3. Stable geometries for the H atom on the Pt/β-Mo_2C surfaces after the relaxation. The colored spheres represent the same atoms as in Figure 1, H atoms are represented by the blue spheres.

On Pt/C-Mo_2C, hydrogen stability is comparable to that on Pt(111) surface, however, atomic hydrogen here interacts with the surface mainly through the formation of C–H bond as mentioned above (Figure 3), while in Pt/Mo-Mo_2C system the H–surface interaction is weaker, evidenced from E_{ads} 0.3 eV lower than on Pt(111). Forming C–H bond appears to be an important factor in atomic hydrogen stabilization on the Pt/C-Mo_2C surface. Indeed, the adsorption energy on the second most stable adsorption site for H on this surface, namely E*hcp*, is -0.33 eV and is closer to the value on the most stable site in the Pt/Mo-Mo_2C system.

Table 2. Adsorption energy (E_{ads}), average H–nearest surface atom distance (d(H-Pt)), average shortest H–surface distance (d⊥(H-Pt)) and Bader charge values (Q) for atomic hydrogen adsorbed on the Pt/TMC surface.

System	Site	E_{ads} (eV)[a]	d(H-Pt) (Å)[b]	d⊥(H-Pt) (Å)[b]	Q (*e*)
Pt/C-Mo_2C	C*hcp*	-0.62	1.11	1.11	+0.11
Pt/Mo-Mo_2C	Mo*hcp*	-0.29	1.87	~ 0	-0.07
Pt/C-WC	C*hcp*	0.64	1.82	1.10	-0.10
Pt/W-WC	Top	-0.60	1.80	1.80	-0.10
Pt(111)	E*hcp*	-0.59	1.87	1.07	-0.05

[a]Values in parentheses correspond to the adsorption energy calculated, using $\frac{1}{2}E_{H_2}$ as the reference

[b]d corresponds to the distance between the adsorbate and the closest surface atom; d⊥ is the shortest normal distance from the adsorbate to the surface plane.

From the data presented, it is clear that the presence of the W-WC support has a small to negligible effect on H adsorption at low coverage, compared to pristine Pt(111); while for C-termination of the support, hydrogen adsorption energies are slightly larger than on Pt(111), which have already been reported, although with a larger difference between hydrogen adsorption energies on Pt monolayer, supported on C-WC and W-WC [17,18]. The work of Esposito *et al.* [10], suggests that on the W-terminated support a weakening of the H–Pt interaction occurs, evidenced by adsorption energies 0.13 eV lower than on Pt(111), while in this work H adsorption on Pt is almost not affected by the presence of the support, regardless of its termination. Similar conclusions have been made by Vasić *et al.* [17] and Anićijević *et al.* [18], and small differences between the current work and previously reported observations may be a result of employing different modeling approaches, similarly to those, mentioned above for H adsorption on pristine Pt(111). Furthermore, a variation of 0.1-0.15 eV is well within the error limit of this type of calculations and it will be almost irrelevant for experiments done at room temperature.

Weaker adsorption of atomic hydrogen on Pt/β-Mo_2C, as compared to Pt/α-WC at low coverage of 1/9 ML, has been reported by Zhang *et al.*, who found a difference of 0.14 eV between the adsorption energies of hydrogen on these surfaces [56] (although not specifying termination of the TMC), possibly a result of a slight increase of Pt–Pt distances in the monolayer, mentioned above. Stable atomic hydrogen adsorption on Pt/α-WC and Pt/C-Mo_2C, comparable to adsorption on Pt(111) is somewhat unexpected, taking into account the downshift of Pt *d*-band center, discussed earlier. However, additionally to the changes in the electronic structure of the supported monolayer, there are other factors defining the stability of the adsorbate on the supported surfaces, such as involvement of the support into surface–adsorbate charge transfer as reported previously [36]. It has been shown clearly that even when a downshift of a surface *d*-band center takes place, the adsorbate can be stabilized if it is able to acquire a negative charge from the surface [36] Therefore, the adsorption energy for H on Pt/α-WC surfaces can be seen as a function of two factors: position of the *d*-band center of the supported monolayer and total net charge acquired by the adsorbate. Even though the *d*-band center downshift would imply a weaker adsorbate–surface interaction, a large enough net charge acquired by the adsorbate would lead to its stabilization.

From this perspective it can be seen that net charge, acquired by H atom adsorbed on Pt/α-WC(0001) surfaces is -0.10 *e* (Table 2), which is twice of its net charge on Pt(111). On Pt/W-WC, H is able to acquire this charge from Pt monolayer that already has a surplus; although in Pt/C-WC system Pt monolayer cedes 0.19 *e* to the support, small separation between the support and the monolayer enable the charge transfer between the adsorbed H and the carbide. This involvement of the C-WC support into the charge transfer from/to the adsorbate, can be appreciated in Figure 4, from which it is clear that the charge distribution on the support's upmost C atoms, the ones closest to the location of the H atom, is affected by the adsorbate's presence.

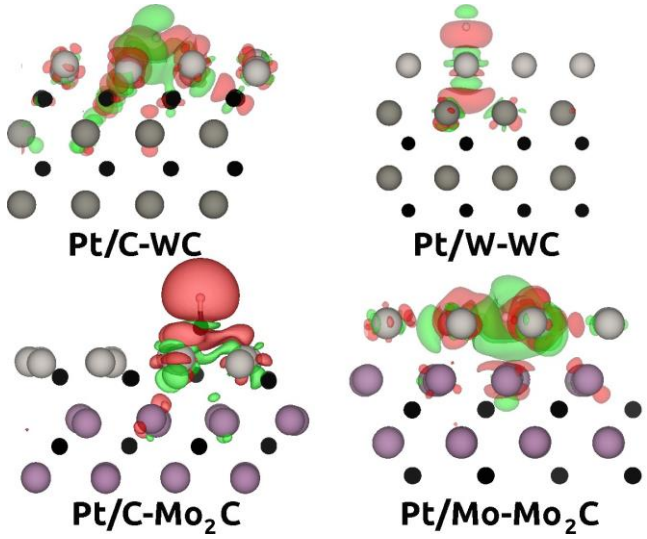

Figure 4. Charge density difference (CDD) plots for a H atom adsorbed on Pt/TMC surfaces. Green and red regions correspond to a charge loss (atoms become more positively charged) and charge accumulation (atoms become more negatively charged), respectively.

Upon H adsorption on Pt/C-Mo_2C, the adsorbate loses a small charge (+0.11 *e*) due to the formation of the C–H bond similarly to what has been observed for systems with surface carbon atoms available for interaction [35,58]. On Pt/Mo-Mo_2C, the total charge acquired by a H atom is slightly larger than that on Pt(111), and the downshift of the Pt ML *d*-band is quite small (-2.63 vs. -2.58 eV on Pt(111)). These descriptors should not contribute significantly to the weakening of the H–Pt interaction; therefore, these factors do not explain the $E_{ads,H}$ value calculated for this surface. Therefore the overall lower H–Pt interaction on Pt/Mo-Mo_2C must be attributed to the reorganization of the surface geometry upon atomic hydrogen adsorption and the fact that it interacts not only with Pt atoms of the monolayer but also directly with the support, suggesting that these factors must be taken into account when evaluating the HER activity of this system.

The obtained results clearly evidence that the stability of atomic hydrogen on supported platinum depends on the support, *i.e.* the type of carbide and their terminations, which was in direct contact with the Pt monolayer. Consequently, electrocatalytic activity of these composite systems towards HER would vary with TMC support and its termination.

3.3 Pt/TMC activity for HER at low H coverage

In the context of the catalytic properties for HER, knowing $E_{ads,H}$ values can be extremely useful for a preliminary theoretical assessment of electrocatalytic activity of materials for HER, since the hydrogen-metal bonding energy can be used as a descriptor of activity [3-5,55].

The idea behind using $E_{ads,H}$ as a descriptor for HER activity relies in the Sabatier's principle [66]. The reactants and intermediates have to bind to the surface of the catalyst strong enough in order to promote the reaction, however, not too strong to avoid surface blockage. For the case of HER, the surface should bind atomic hydrogen strongly enough to promote the reaction and weakly enough, so the desorption of the reaction product (H_2) would be possible. Therefore there exists some optimal value of $E_{ads,H}$, that assures optimal catalytic activity.

HER exchange current density is a commonly used experimental criterion for evaluating catalytic activity of a material towards HER. Plotting it against the value of $E_{ads,H}$, a volcano-type curve is obtained in such a way that the materials with the best catalytic properties for HER are located in the proximity of an apex of the curve. Although underlying principles are not completely clear yet, HER volcano plot is a useful tool, as a first approximation, for screening potential new catalysts, actively used throughout the literature.

To construct a volcano curve, hydrogen adsorption energies have been obtained for the 12 metals used in work of Nørskov *et a.l* [3], using exactly the same model setup as described in the Computation Details section (listed in Table S6). Experimental values for HER exchange current density were taken from the above mentioned report of Nørskov *et al.*[3] and Trasatti [5] and were plotted versus the corresponding $E_{ads,H}$. Two branches of volcano curve were fitted with linear functions, and in numerical form, they can be written as

$$\mathrm{Log}(i_o/\mathrm{A\,cm^{-2}}) = \begin{cases} 4.855 + 14.322 \cdot E_{ads,H}, E_{ads,H} < -0.59\,\mathrm{eV} \\ -7.617 - 7.055 \cdot E_{ads,H}, E_{ads,H} \geq -0.59\,\mathrm{eV} \end{cases} \qquad (13)$$

The resulting plot can be appreciated in Figure 5. The Pt/TMC systems were placed on the obtained volcano curve by locating the intersection of the predicted side of the curve with corresponding $E_{ads,H}$ value (Table 2) and predicted values of Log (i_0/A cm^{-2}) for Pt/TMC system are summarized in Table S4.

Analyzing the curve it is important to notice that neither of the investigated Pt/TMC systems exceeds the activity of Pt(111) surface toward HER. Nonetheless, Pt/W-WC system is located very close to the apex of the curve (Log i_0 is -3.67 A cm^2), suggesting an activity very close to that of Pt, in agreement with experimental observations [14,10], while Pt/C-WC appears to be slightly less active.

From the positions of the studied systems on the volcano curve it is seen that Pt monolayers on the terminations of the α-WC(0001) support are expected to have a higher activity than Pt/β-Mo_2C systems. It is important to note that the estimated exchange density for Pt/β-Mo_2C systems is -3.97 and -5.45 A cm^2 for C- and Mo-terminated support, respectively, while the experimental value of -3.2 A cm^2 has been reported [15]. While obviously underestimating the real electrocatalytic activity of Pt/β-Mo_2C the obtained results firmly indicate that β-Mo_2C

is a viable material to be used as support for Pt-based HER catalysts. Thus, information derived from the volcano curve for composite systems comprised of an active metal monolayer and TMC support can be used for the preliminary theoretical evaluation of such materials towards the HER.

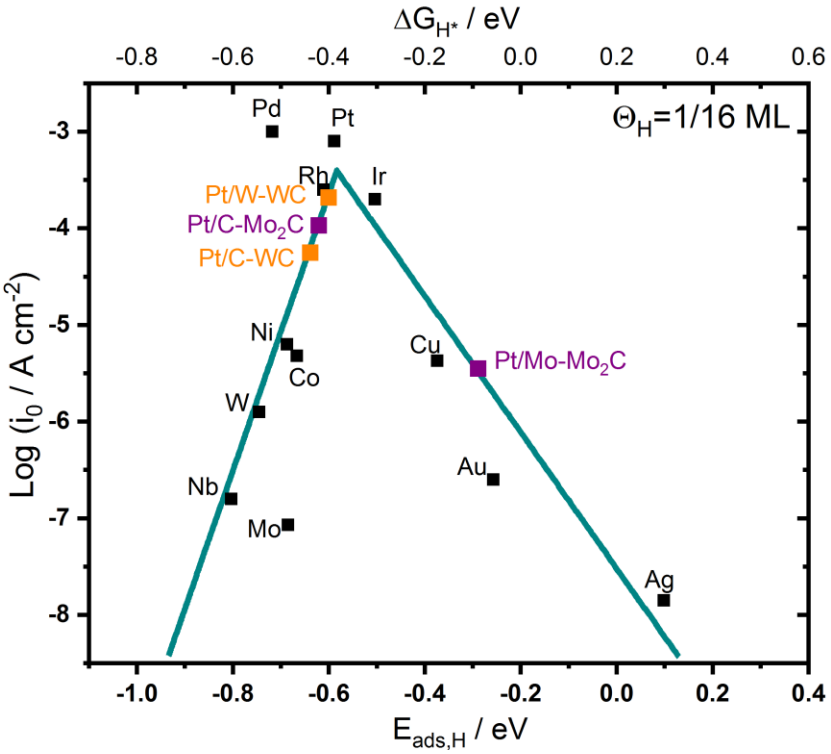

Figure 5. Volcano curve showing the correlation between theoretically calculated adsorption energy of atomic hydrogen and experimentally obtained HER exchange current densities for selected metals. Free energies for hydrogen adsorption, ΔG_{H^*}, calculated as $E_{ads,H}$ + 0.24 eV [3], are indicated as well. Predictions for the HER activity of Pt/α-WC and Pt/β-Mo_2C systems are indicated with orange and purple squares, respectively.

In a realistic Pt/TMC system, the actual termination of the support is unknown and is a contribution of statistical proportions of C- and M-terminated surfaces, which mainly depend on the chosen synthesis protocol. From the obtained volcano curve, it appears that the predicted values of Log i_0 for Pt/W-WC and Pt/C-Mo_2C are closer to the experimental values than those predicted for Pt/C-WC and Pt/Mo-Mo_2C. However, it will be wrong to assume that in real Pt/TMC systems, reported in the literature, Pt/W-WC and Pt/C-Mo_2C are the prevailing components in the synthesized Pt/α-WC and Pt/β-Mo_2C materials, respectively, because reported experimental values can the sum of several factors, such as Pt/TMC synthesis protocol, location of the adsorbed hydrogen on these surfaces [67] and the platinum structure on the TMC support itself .

Therefore, it is possible to use the volcano curve for a preliminary assessment of electrocatalytic activity for a selected material. However, one should keep in mind that there are particular features, which can have an impact on the resulting catalytic activity; this applies especially when analyzing complex systems.

In the case of the Pt/TMC systems, for instance, an average activity predicted for different terminations of the support could be used. However, as it can be easily seen, underestimation of the activity, introduced by including Pt/C-WC and Pt/Mo-Mo_2C would lead to the values of Log i_0 lower than experimental ones. Thus, after the initial evaluation of the activity towards HER, an actual electrochemical experiment must be conducted to obtain a conclusive data.

3.4 Coverage-dependent H adsorption on Pt/TMC and impact of Θ_H on their predicted HER activity

An experimental study by Marcović and Ross estimated that the hydrogen coverage on the Pt(111) electrode is 2/3 of a ML at the equilibrium potential [6]. Thus, studying atomic hydrogen adsorption on Pt(111) and Pt/TMC surfaces at higher coverages may not describe rigorously the actual situation in the experiment. Nonetheless, using the same reasoning as in the work of Hamada and Morikawa [68], at a fundamental level, it is of interest to include the effect of the coverage in a study of the hydrogen interaction with TMC-supported platinum surfaces, considering low and high values in Θ_H, and compare the results with the those obtained on unsupported Pt(111).

For this purpose, Pt/TMC surfaces with a number of H atoms ranging from 1 to 16 have been tested. Special attention has been paid to the systems with 8 and 16 H atoms as they correspond to Θ_H of 1/2 and 1 hydrogen ML, respectively. It must be noted here that these growing coverages have been modeled by adsorbing all hydrogen atoms onto the most stable sites of the Pt/TMC surfaces, described above, mirroring previous works on coverage-dependent hydrogen adsorption on Pt surfaces [68-70]. In the particular case of Pt/C-Mo_2C systems, when the preferable C*hcp* adsorption sites are all filled after reaching coverages larger than half a monolayer of hydrogen, additional adsorbate atoms were placed on E*hcp* sites. A similar approach was used by Gudmundsdottir *et al.* in their study for coverage-dependent H adsorption on Pt(110) surface, where after saturation of the most stable sites, hydrogen adsorption occurred on the next-stable sites[45].

To get an idea about changes in the geometry of the Pt/TMC systems caused by higher hydrogen coverage, one can take the geometry of each H-Pt/TMC system at the coverages 1/2 and 1 ML, remove all hydrogen atoms and obtain its total energy from a single-point calculation. Comparing these energies to a reference energy of the same system at 1/16 ML coverage, provides a measurable extent of the changes in the Pt/TMC surface. The obtained geometries are shown in Figure 6.

From these calculations (Table S5), it has been estimated that Pt/C-Mo_2C and Pt/C-WC are the systems whose geometries were affected the most by increasing hydrogen coverage, followed by Pt/Mo-Mo_2C, while the geometry of Pt/W-WC remains almost unchanged.

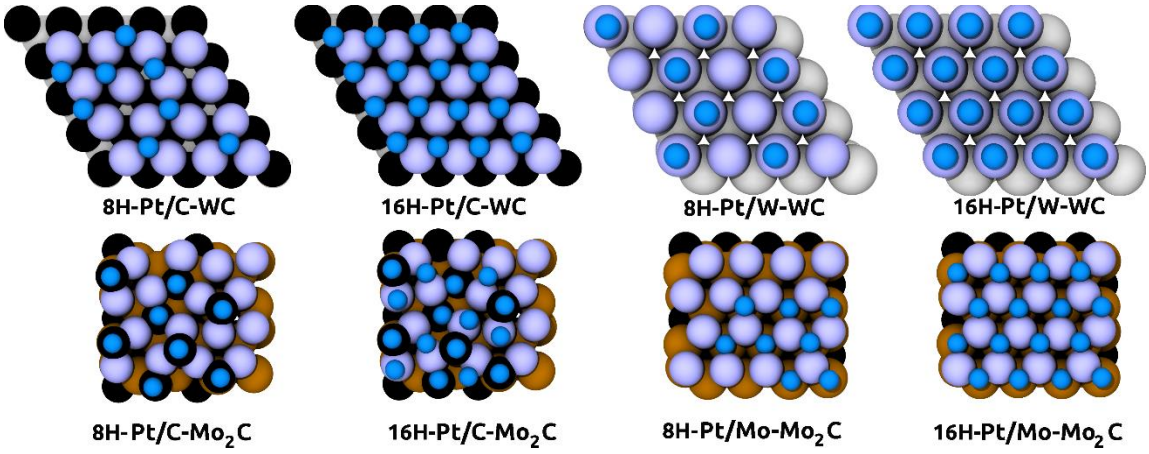

Figure 6. Stable geometries for atomic H coverages of 1/2 and 1 ML on the Pt/TMC surfaces obtained after relaxation of their structures. The colored spheres represent the same atoms as in Figure 3.

For the particular case of a Pt/C-Mo_2C system, where the difference between total energies of the surface at each increase of Θ_H is close to 4 eV, a distortion of its geometry can be seen already with 8 H atoms present on the surface and this deformation becomes more visible when Θ_H reaches 1 ML. This deformation of the supported Pt monolayer can be explained having in mind that the preferable adsorption site for atomic hydrogen on this surface is C*hcp* and that upon H adsorption a C–H bond is formed which causes the support's C atom to come from underneath of the supported monolayer to a position above it (See Figure 3). Furthermore while at Θ_H = 1/2 there are enough C*hcp* sites to accommodate all adsorbed H atoms, at a monolayer coverage, due to the fact that there are only 8 C atoms of β-Mo_2C available for the adsorption, hydrogen is forced to adsorb on sites that at the lower coverages are unfavorable. Somewhat similar change in the adsorption location has been reported for hydrogen at high coverage on TiC(001) [59] and δ-MoC(001) [71].

Stepwise adsorption energies, calculated from eq. 9, plotted against Θ_H can be seen in Figure 7. For comparison, $E_{ads,H}$ values on plain Pt(111) were plotted as well.

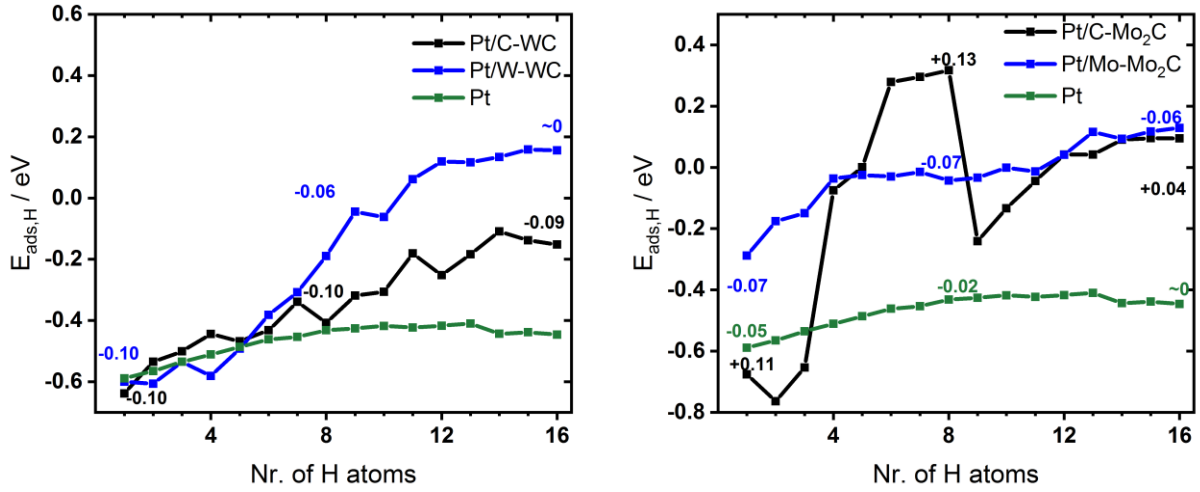

Figure 7. Stepwise $E_{ads,H}$ on plain Pt and Pt/TMC surfaces as a function of the number of H atoms in the unit cell. For systems with hydrogen coverages of 1/16, 1/2 and 1 ML, an average Bader charge on the H atoms is indicated. [Question: In the left side panel, blue curve, the value at the top is just "-0"? Or "-0.00"?

On Pt/α-WC surfaces, increasing the number of H atoms, expectedly, weakens their adsorption energy due to repulsive hydrogen–hydrogen Pauli interactions, regardless of the support's termination. However, the overall difference between the $E_{ads,H}$ at Θ_H = 1/16 and at 1 ML coverage is greater in the Pt/W-WC system than in the Pt/C-WC (~ 0.8 and ~ 0.5eV, respectively).

By analyzing the variation in the average net charge on H atoms with growing Θ_H it becomes clear that in Pt/C-WC system changes in the average net charge are minimal, and therefore weaker H adsorption at higher coverages is only caused by the repulsive hydrogen–hydrogen interactions. On the other hand, in the Pt/W-WC system, the average net charge on H atoms decreases steadily with the growing coverage, indicating that additionally to the repulsive interactions between co-adsorbed H atoms, a significant weakening in H–Pt interaction takes place.

In Figure 7, the most interesting feature seen in the case of atomic H adsorption on the Pt/β-Mo_2C support is the $E_{ads,H}$ climbing with hydrogen coverage on the Pt/C-Mo_2C surface until it reaches the value of 1/2 ML, after which a significant drop is observed. The overall difference between the adsorption energies at lowest 1/16 ML coverage and 1 ML coverage is close to 0.7 eV. Furthermore, it can be clearly seen that most of the decrease in $E_{ads,H}$ occurs at coverages less than 1/2 ML, which is explained by the saturation of the available C*hcp* sites described above. This conclusion is also supported by the analysis of net charge per H atom (obtained by averaging net charge of each H at a given coverage), where it can be appreciated that H atoms keep ceding the charge to the surface due to the strong C–H interaction, until Θ_H reaches 1/2 ML, therefore, weakening surface–H bonding. After that, there are no C atoms available, and the H–Pt interaction becomes dominant, leading to a much smaller variations in the $E_{ads,H}$. Interestingly, at Θ_H > 1/2 ML, the net charge on the H atoms adsorbed on

the C*hcp* sites is -0.05 *e*, contributing to the decrease in the positive average net charge from +0.13 to +0.04 *e* when going from 1/2 ML coverage to 1ML.

Finally, a comparably small change in $E_{ads,H}$ with the H coverage (~0.4 eV between the energies of the systems with lowest and highest hydrogen coverages) have been observed for the Pt/Mo-Mo_2C system, which is due to the combination of the availability of the preferred Mo*hcp* sites for H adsorption and the significant separation between H atoms on this surface, that reduces the repulsive lateral H-H interaction on this substrate. Indeed the average H-H distance on Pt/Mo-Mo_2C is 3.15 Å, which is the highest compared to the rest of the studied Pt/TMC surfaces (2.81, 2.82, 2.93 and 2.35 Å on Pt/ Pt/C-WC, Pt/W-WC and Pt/C-Mo_2C, respectively). Combined with the average net charge on the H atoms that remains almost constant with the growing coverage, it resulted in the smallest variation of stepwise $E_{ads,H}$ with coverage among the studied Pt/TMC surfaces.

At the same time, the stepwise adsorption energy on Pt(111) surface does not vary significantly with the surface coverage and the difference between the stepwise adsorption energies at the lowest and highest surface coverages is ~0.1 eV, between the average adsorption energies is ~0.1 eV which has been reported before and explained by the small lateral H-H interaction on this surface [68,69].

In order to explain the origins of the variations of the $E_{ads,H}$ with the surface coverage on Pt/TMC surfaces, stepwise adsorption energies were plotted against the coverage for the metal surfaces used to obtain the volcano plot as well as for pristine α-WC(0001) and β-Mo_2C(100) surfaces (Figure 8).

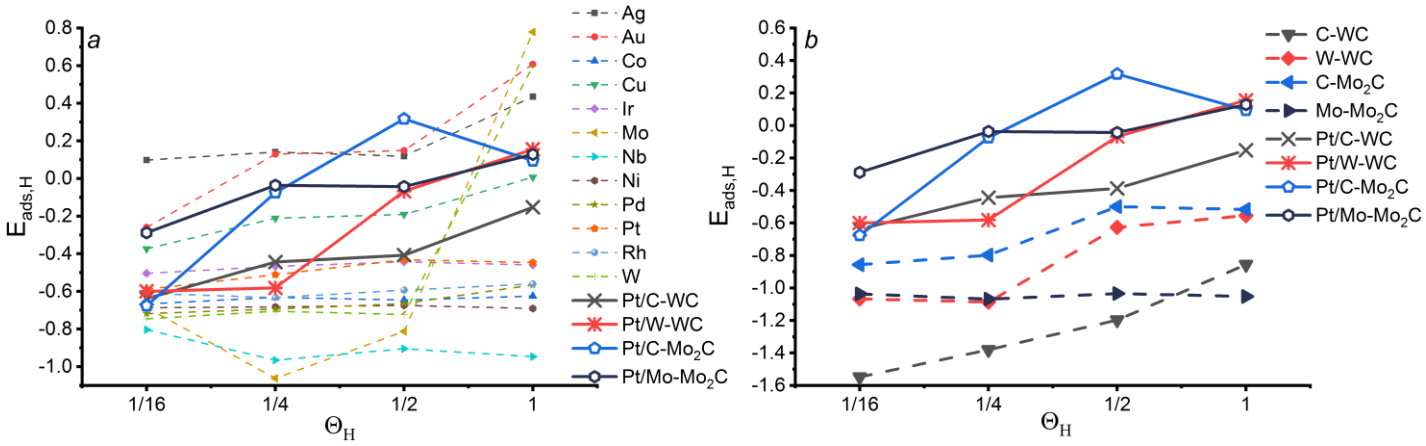

Figure 8. Variation in stepwise atomic hydrogen adsorption energies with Θ_H on (a) metal surfaces (dashed lines) and Pt/TMC (straight lines); (b) TMC (dashed lines) and Pt/TMC (straight lines).

The choice of metal surfaces for this analysis is dictated by the wide variability in properties of the metals in this selection, including high and low HER activity.

Analyzing closely the tendencies seen in Figure 8(a), it becomes evident that, depending on where in the Periodic Table the metal is found, a different dependency of $E_{ads,H}$ on the coverage is seen. On Nb (group 5) the increasing coverage leads to strengthening of H-surface interactions; on metals from groups 9 (Co, Rh, Ir) and 10

(Ni, Pd, Pt) no significant changes are observed in the stability of atomic H with increasing Θ_H; on group 11 metal surfaces (Cu, Ag, Au) a comparatively moderate weakening of H-surface interactions is seen; and, finally, group 6 (W, Mo) are the metals where at intermediate coverages a hydrogen stabilization occurs and going to 1 ML coverage a dramatic drop in H stability takes place.

Comparing the observed trends on Pt/TMC surfaces to those on the Pt(111) surface and on the corresponding pristine terminations of the support in each case, it is clear that the way how the adsorption energy changes with the coverage on the supported Pt surfaces is closer to the corresponding carbide termination than to Pt(111). In this regard, it has been reported that for supported metals, the thickness at which properties of the supported layer start to fully resemble properties of the metal surfaces, depends on the nature of the metal [Trasatti S. The electrode potential. In: Bokris J. O'M., Conway B. E., Yeager E. Comprehensive treatise of electrochemistry. Volume 1: Double layer. Springer Science + Business Media, New York, 1980, 45-83]. For platinum, just a monolayer coverage is not enough to recreate fully the properties of the supported metal and few monolayers are required.

Therefore in the case of Pt/TMC systems with a monolayer coverage of Pt, the changes in $E_{ads,H}$ with the Θ_H are controlled by the nature of the support rather than by the supported platinum. In its turn, the effect of Pt on hydrogen stability in Pt/TMC in respect to H-TMC systems consists in weakening of H-surface interactions by shielding the TMC surfaces which by themselves tend to over-bind atomic H [10,35,55].

Interestingly, the fact that the hydrogen adsorption energy on some metallic surfaces does not change significantly with the total number of hydrogen atoms, suggests that plotting the experimentally observed exchange current densities against hydrogen adsorption energies at low 1/16 ML coverage and at 1 ML coverage should not change noticeably the overall trends of the HER activity for simple metal surfaces. Indeed, Nørskov *et al.* already reported the conservation of the activity trends regardless of the coverage on the surfaces, used for deriving the volcano curve [3]. From the Figures 7 and 8, however, it is evident that adsorption energies on Pt/TMC surfaces vary with the coverage, thus the volcano curves calculated from hydrogen adsorption energies on metal surfaces at different coverages may predict a different HER activity of the Pt/TMC surfaces. The significance of this observation for the theoretical screening of complex materials such as Pt/TMC is that a possibility exists to underestimate the HER activity of an analyzed system if the coverage was not low enough.

To verify this hypothesis, it is not sufficient to simply recalculate the hydrogen adsorption energy in the Pt/TMC at different Θ_H and place them on the volcano curve from Figure 5, but the whole volcano curve must be obtained at the same coverage. For any interested reader, a detailed description of the method used to obtain the higher-coverage volcano curves and their analysis is available in Section S2 of Supplemental Information.

On the resulting plots, presented in Figure S7 it can be seen that compared to the volcano plot at the low 1/16 ML coverage (Figure 5), the overall activity trends indeed remain the same, while the position of the Pt/TMC systems changes, mainly because of the larger variations in $E_{ads,H}$ on the that on Pt/TMC compared to that on the extended metal surfaces (see Figure S8 and Table S6).

Our calculations confirm that for simple systems such as extended metal surfaces, the effect of atomic hydrogen coverage does not play a significant role on their positions on the volcano curve, which, itself, does not change significantly with Θ_H, preserving activity trends. For more complex materials, such as Pt monolayer supported on TMC, only exchange current densities predicted from the volcano curve calculated at low 1/16 ML coverage are the closest to experimentally observed values for Pt ML on both WC and Mo_2C supports, while higher-coverage curves predict lower activity than the experimentally observed for systems such as Pt/C-Mo_2C and Pt/W-WC.

Atomic hydrogen stability in these systems depends significantly on Θ_H, and the position of the system on the volcano curve is a function of the hydrogen coverage at which the adsorption energies used to derive the volcano curve were calculated. This observation evidences that in order to correctly asses the HER activity of a system of interest, the atomic hydrogen adsorption energy should be calculated at different values of Θ_H and its variation with the coverage must be assessed.

4 Conclusions

Periodic DFT calculations have been carried out on a Pt monolayer supported on α-WC(0001) and β-Mo_2C(100) surfaces to investigate atomic hydrogen adsorption over the Pt/TMC systems. The obtained information demonstrate that for the studied Pt/TMC systems, the structural and electronic properties of the supported monolayer depend on the intrinsic nature of the carbide and its surface terminations and define how the resulting Pt/TMC material interacts with atomic hydrogen, and its overall HER activity.

The present study confirms that at low H coverage Pt/α-WC surfaces interact with atomic hydrogen similarly to a plain Pt(111) substrate. At the same time, hydrogen differently with Pt/C-Mo_2C, compared to the Pt/Mo-Mo_2C surface, mainly because of the formation of C–H bonds with the carbon atoms of the support. After being placed on the volcano curve, all four systems show quite high predicted activity for the HER.

Nonetheless, values of the exchange current densities for Pt/W-WC and Pt/C-Mo_2C systems closer to the experimentally measured results, than those for Pt/C-WC and Pt/Mo-Mo_2C, indicate, that for complex materials such as Pt/TMC, the volcano curve method is a useful tool for only an initial theoretical screening of potential catalysts for HER. To confirm or refute conclusively, the predicted HER activity an actual electrochemical study is still required.

An analysis of atomic hydrogen adsorption on Pt/TMC at different surface coverages showed a striking difference between TMC-supported Pt monolayers and low index metal surfaces, specifically in the variability of atomic H stability with hydrogen coverage. It has been explained by insufficiency of a single Pt monolayer to completely resemble the properties Pt(111) surface and the conclusion was made that this dependency of $E_{ads,H}$ on the surface coverage is driven by the nature of the support in the Pt/TMC systems.

The variability of the hydrogen adsorption energy with the coverage on the Pt/TMC suggests that the theoretical evaluation of HER activity for similar systems is advised to be done only after verifying whether a dependency of $E_{ads,H}$ on Θ_H is present, to avoid introducing an error in the results.

In summary, the obtained information may be used in further studies dedicated to theoretical evaluation of electrocatalytic activity of the complex supported metal/support systems and have a potential use for the field of controlled design of catalytically active materials.

Acknowledgements

Authors would like to thank the Universidad de Medellín, UdeM, (A. Koverga, E. Florez, and C. Jimenez-Orozco), for the financial support under the internal project 1110. The work done at the Chemistry Department of BNL (J. A. Rodriguez) was supported by the U.S. DOE Office of Basic Energy Sciences under Contract No. DE-SC0012704. Part of this research used resources of the Center for Functional Nanomaterials, which is a U.S. DOE Office of Science Facility, and the Scientific Data and Computing Center, a component of the Computational Science Initiative, at Brookhaven National Laboratory under Contract No. DE-SC0012704.

References

1. D.H. Youn, S. Han, J.Y. Kim, J.Y. Kim, H. Park, S.H. Choi, J.S. Lee, Highly active and stable hydrogen evolution electrocatalysts based on molybdenum compounds on carbon nanotube-graphene hybrid support, ACS Nano. 8 (2014) 5164–5173.
2. Y. Zheng, Y. Jiao, M. Jaroniec, S.Z. Qiao, Advancing the electrochemistry of the hydrogen- Evolution reaction through combining experiment, Angew. Chemie - Int. Ed. 54 (2015) 52–65.
3. J.K. Nørskov, T. Bligaard, A. Logadottir, J.R. Kitchin, J.G. Chen, S. Pandelov, U. Stimming, Trends in the Exchange Current for Hydrogen Evolution, J. Electrochem. Soc. 152 (2005) J23.
4. B.E. Conway, J.O. Bockris, Electrolytic Hydrogen Evolution Kinetics and Its Relation to the Electronic and Adsorptive Properties of the Metal, J. Chem. Phys. 26, (1957) 532–541.
5. S. Trasatti, Work function, electronegativity, and electrochemical behaviour of metals. III. Electrolytic hydrogen evolution in acid solutions, J. Electroanal. Chem. 39 (1972) 163–184.
6. N. Marković P. N. Ross, Surface science studies of model fuel cell electrocatalysts, Surf. Sci. Rep. 45 (2002) 117–229.
7. C.-J. Yang, An impending platinum crisis and its implications for the future of the automobile, Energy Policy. 37 (2009) 1805–1808.
8. R.B. Gordon, M. Bertram, T.E. Graedel, Metal stocks and sustainability, Proc. Natl. Acad. Sci. U. S. A. 103 (2006) 1209–1214.

9. D. V. Esposito, S.T. Hunt, A.L. Stottlemyer, K.D. Dobson, B.E. McCandless, R.W. Birkmire, J.G. Chen, Low-Cost Hydrogen-Evolution Catalysts Based on Monolayer Platinum on Tungsten Monocarbide Substrates, Angew. Chemie Int. Ed. 49 (2010) 9859–9862.
10. D. V. Esposito, S.T. Hunt, Y.C. Kimmel, J.G. Chen, A New Class of Electrocatalysts for Hydrogen Production from Water Electrolysis: Metal Monolayers Supported on Low-Cost Transition Metal Carbides, J. Am. Chem. Soc. 134 (2012) 3025–3033.
11. R.B. Levy, M. Boudart, Platinum-like behavior of tungsten carbide in surface catalysis, Science (80-.). 181 (1973) 547–549.
12. M.C. Weidman, D. V. Esposito, Y.-C. Hsu, J.G. Chen, Comparison of electrochemical stability of transition metal carbides (WC, W2C, Mo2C) over a wide pH range, J. Power Sources. 202 (2012) 11–17.
13. A.M. Gómez-Marín, E.A. Ticianelli, Analysis of the electrocatalytic activity of α-molybdenum carbide thin porous electrodes toward the hydrogen evolution reaction, Electrochim. Acta. 220 (2016) 363–372.
14. D. V. Esposito, J.G. Chen, Monolayer platinum supported on tungsten carbides as low-cost electrocatalysts: opportunities and limitations, Energy Environ. Sci. 4 (2011) 3900.
15. T.G. Kelly, K.X. Lee, J.G. Chen, Pt-modified molybdenum carbide for the hydrogen evolution reaction: From model surfaces to powder electrocatalysts, J. Power Sources. 271 (2014) 76–81.
16. C. Ma, T. Liu, L. Chen, A computational study of H_2 dissociation and CO adsorption on the Pt_{ML}/WC(0001) surface, Appl. Surf. Sci. 256 (2010) 7400–7405.
17. D.D. Vasić, I.A. Pašti, S. V. Mentus, DFT study of platinum and palladium overlayers on tungsten carbide: Structure and electrocatalytic activity toward hydrogen oxidation/evolution reaction, Int. J. Hydrogen Energy. 38 (2013) 5009–5018.
18. D.D. Vasić Anićijević, V.M. Nikolić, M.P. Marčeta-Kaninski, I.A. Pašti, Is platinum necessary for efficient hydrogen evolution? - DFT study of metal monolayers on tungsten carbide, Int. J. Hydrogen Energy. 38 (2013) 16071–16079.
19. A.S. Kurlov, A.I. Gusev, Tungsten Carbides. Structure, Properties and Application in Hardmetals, Springer International Publishing, 1st edn, 2013, pp. 5–56.
20. C. Jimenez-Orozco, E. Florez, A. Moreno, P. Liu, J.A. Rodriguez, Acetylene and Ethylene Adsorption on a β-Mo 2 C(100) Surface: A Periodic DFT Study on the Role of C- and Mo-Terminations for Bonding and Hydrogenation Reactions, J. Phys. Chem. C. 121 (2017) 19786–19795.
21. J.R. dos S. Politi, F. Viñes, J.A. Rodriguez, F. Illas, Atomic and electronic structure of molybdenum carbide phases: bulk and low Miller-index surfaces, Phys. Chem. Chem. Phys. 15 (2013) 12617.
22. S. Posada-Pérez, F. Viñes, P.J. Ramirez, A.B. Vidal, J.A. Rodriguez, F. Illas, The bending machine: CO_2 activation and hydrogenation on δ-MoC(001) and β-Mo2C(001) surfaces, in: Phys. Chem. Chem. Phys., Royal Society of Chemistry, 2014: pp. 14912–14921.

23. S. Posada-Pérez, P.J. Ramírez, R.A. Gutiérrez, D.J. Stacchiola, F. Viñes, P. Liu, F. Illas, J.A. Rodriguez, The conversion of CO_2 to methanol on orthorhombic β-Mo_2C and Cu/β-Mo_2C catalysts: Mechanism for admetal induced change in the selectivity and activity, Catal. Sci. Technol. 6 (2016) 6766–6777.
24. G. Kresse, J. Hafner, Ab initio molecular dynamics for liquid metals, Phys. Rev. B. 47 (1993) 558–561.
25. G. Kresse, J. Hafner, Ab initio molecular-dynamics simulation of the liquid-metalamorphous- semiconductor transition in germanium, Phys. Rev. B. 49 (1994) 14251–14269.
26. G. Kresse, J. Furthmüller, Efficient iterative schemes for ab initio total-energy calculations using a plane-wave basis set, Phys. Rev. B - Condens. Matter Mater. Phys. 54 (1996) 11169–11186.
27. G. Kresse, J. Furthmüller, Efficiency of ab-initio total energy calculations for metals and semiconductors using a plane-wave basis set, Comput. Mater. Sci. 6 (1996) 15–50.
28. J.P. Perdew, K. Burke, M. Ernzerhof, Generalized gradient approximation made simple, Phys. Rev. Lett. 77 (1996) 3865–3868.
29. P.E. Blöchl, Projector augmented-wave method, Phys. Rev. B. 50 (1994) 17953–17979.
30. D. Joubert, From ultrasoft pseudopotentials to the projector augmented-wave method, Phys. Rev. B - Condens. Matter Mater. Phys. 59 (1999) 1758–1775.
31. S. Grimme, Accurate description of van der Waals complexes by density functional theory including empirical corrections, J. Comput. Chem. 25 (2004) 1463–1473.
32. S. Grimme, J. Antony, S. Ehrlich, H. Krieg, A consistent and accurate ab initio parametrization of density functional dispersion correction (DFT-D) for the 94 elements H-Pu, J. Chem. Phys. 132 (2010) 154104.
33. H.J. Monkhorst, J.D. Pack, Special points for Brillouin-zone integrations, Phys. Rev. B. 13 (1976) 5188–5192.
34. M. Methfessel, A.T. Paxton, High-precision sampling for Brillouin-zone integration in metals, Phys. Rev. B. 40 (1989) 3616–3621.
35. A.A. Koverga, E. Flórez, L. Dorkis, J.A. Rodriguez, CO, CO2, and H2 Interactions with (0001) and (001) Tungsten Carbide Surfaces: Importance of Carbon and Metal Sites, J. Phys. Chem. C. 123 (2019) 8871–8883.
36. A.A. Koverga, E. Flórez, L. Dorkis, J.A. Rodriguez, Promoting effect of tungsten carbide on the catalytic activity of Cu for CO2 reduction, Phys. Chem. Chem. Phys. 22 (2020) 13666–13679.
37. S. Posada-Pérez, F. Viñes, J.A. Rodríguez, F. Illas, Structure and electronic properties of Cu nanoclusters supported on Mo2C(001) and MoC(001) surfaces, J. Chem. Phys. 143 (2015) 114704.
38. R. F. W. Bader, *Atoms in Molecules: A Quantum theory*; Oxford University Press: Oxford, U.K., 1990.
39. G. Henkelman, A. Arnaldsson, H. Jónsson, A fast and robust algorithm for Bader decomposition of charge density, Comput. Mater. Sci. 36 (2006) 354–360.
40. A.A. Koverga, S. Frank, M.T.M. Koper, Density Functional Theory study of electric field effects on CO and OH adsorption and co-adsorption on gold surfaces, Electrochim. Acta. 101 (2013) 244–253.

41. K. Momma, F. Izumi, VESTA 3 for three-dimensional visualization of crystal, volumetric and morphology data, J. Appl. Crystallogr. 44 (2011) 1272–1276.
42. W. Humphrey, A. Dalke, K. Schulten, VMD: Visual molecular dynamics, J. Mol. Graph. 14 (1996) 33–38.
43. S. Posada-Pérez, F. Viñes, R. Valero, J.A. Rodriguez, F. Illas, Adsorption and dissociation of molecular hydrogen on orthorhombic β-Mo2C and cubic δ-MoC (001) surfaces, Surf. Sci. 656 (2017) 24–32.
44. M. Yu, L. Liu, Q. Wang, L. Jia, B. Hou, Y. Si, D. Li, Y. Zhao, High coverage H2 adsorption and dissociation on fcc Co surfaces from DFT and thermodynamics, Int. J. Hydrogen Energy. 43 (2018) 5576–5590.
45. S. Gudmundsdóttir, E. Skúlason, K.-J. Weststrate, L. Juurlink, H. Jónsson, Hydrogen adsorption and desorption at the Pt(110)-(1×2) surface: experimental and theoretical study, Phys. Chem. Chem. Phys. 15 (2013) 6323.
46. I.A. Pašti, N.M. Gavrilov, S. V. Mentus, Hydrogen Adsorption on Palladium and Platinum Overlayers: DFT Study, Adv. Phys. Chem. 2011 (2011) 1–8.
47. S. Wannakao, N. Artrith, J. Limtrakul, A.M. Kolpak, Catalytic Activity and Product Selectivity Trends for Carbon Dioxide Electroreduction on Transition Metal-Coated Tungsten Carbides, J. Phys. Chem. C. 121 (2017) 20306–20314.
48. J.L.F. Da Silva, C. Stampfl, M. Scheffler, Converged properties of clean metal surfaces by all-electron first-principles calculations, Surf. Sci. 600 (2006) 703–715.
49. C.B. Krishnamurthy, O. Lori, L. Elbaz, I. Grinberg, First-Principles Investigation of the Formation of Pt Nanorafts on a Mo 2 C Support and Their Catalytic Activity for Oxygen Reduction Reaction, J. Phys. Chem. Lett. 9 (2018) 2229–2234.
50. B. Hammer, J.K. Nørskov, Electronic factors determining the reactivity of metal surfaces, Surf. Sci. 343 (1995) 211–220.
51. B. Hammer, J.K. Norskov, Why gold is the noblest of all the metals, Nature. 376 (1995) 238–240.
52. M. Paßens, V. Caciuc, N. Atodiresei, M. Moors, S. Blügel, R. Waser, S. Karthäuser, Tuning the surface electronic structure of a Pt 3 Ti(111) electro catalyst, Nanoscale. 8 (2016) 13924–13933.
53. H. Duan, Q. Hao, C. Xu, Hierarchical nanoporous PtTi alloy as highly active and durable electrocatalyst toward oxygen reduction reaction, J. Power Sources. 280 (2015) 483–490.
54. V. Stamenkovic, B.S. Mun, K.J.J. Mayrhofer, P.N. Ross, N.M. Markovic, J. Rossmeisl, J. Greeley, J.K. Nørskov, Changing the Activity of Electrocatalysts for Oxygen Reduction by Tuning the Surface Electronic Structure, Angew. Chemie. 118 (2006) 2963–2967.
55. R. Michalsky, Y.J. Zhang, A.A. Peterson, Trends in the hydrogen evolution activity of metal carbide catalysts, ACS Catal. 4 (2014) 1274–1278.
56. Q. Zhang, Z. Jiang, B.M. Tackett, S.R. Denny, B. Tian, X. Chen, B. Wang, J.G. Chen, Trends and Descriptors of Metal-Modified Transition Metal Carbides for Hydrogen Evolution in Alkaline Electrolyte, ACS Catal. 9 (2019) 2415–2422.

57. R.A. Olsen, G.J. Kroes, E.J. Baerends, Atomic and molecular hydrogen interacting with Pt(111), J. Chem. Phys. 111 (1999) 11155–11163.
58. F. Silveri, M.G. Quesne, A. Roldan, N.H. de Leeuw, C.R.A. Catlow, Hydrogen adsorption on transition metal carbides: a DFT study, Phys. Chem. Chem. Phys. 21 (2019) 5335–5343.
59. J.J. Piñero, P.J. Ramírez, S.T. Bromley, F. Illas, F. Viñes, J.A. Rodriguez, Diversity of Adsorbed Hydrogen on the TiC(001) Surface at High Coverages, J. Phys. Chem. C. 122 (2018) 28013–28020.
60. W. Zheng, L. Chen, C. Ma, Density functional study of H2O adsorption and dissociation on WC(0001), Comput. Theor. Chem. 1039 (2014) 75–80.
61. Y.J. Tong, S.Y. Wu, H.T. Chen, Adsorption and reaction of CO and H_2O on WC(0001) surface: A first-principles investigation, Appl. Surf. Sci. 428 (2018) 579–585.
62. S. Khoobiar, Particle to Particle Migration of Hydrogen Atoms on Platinum—Alumina Catalysts from Particle to Neighboring Particles, J. Phys. Chem. 68 (1964) 411–412.
63. S.K. Beaumont, S. Alayoglu, C. Specht, N. Kruse, G.A. Somorjai, A Nanoscale Demonstration of Hydrogen Atom Spillover and Surface Diffusion Across Silica Using the Kinetics of CO_2 Methanation Catalyzed on Spatially Separate Pt and Co Nanoparticles., Nano Lett. 14 (2014) 4792–4796.
64. L.R. Merte, G. Peng, R. Bechstein, F. Rieboldt, C.A. Farberow, L.C. Grabow, W. Kudernatsch, S. Wendt, E. Lægsgaard, M. Mavrikakis, F. Besenbacher, Water-mediated proton hopping on an iron oxide surface, Science (80-.). 336 (2012) 889–893.
65. B. Li, W.L. Yim, Q. Zhang, L. Chen, A comparative study of hydrogen spillover on Pd and Pt decorated MoO 3(010) surfaces from first principles, J. Phys. Chem. C. 114 (2010) 3052–3058.
66. P. Sabatier, *La catalyse en chimie organique*; Paris et Liege : Librairie polytechnique, 1920.
67. B.E. Conway, G. Jerkiewicz, Relation of energies and coverages of underpotential and overpotential deposited H at Pt and other metals to the 'volcano curve' for cathodic H2 evolution kinetics, Electrochim. Acta. 45 (2000) 4075–4083.
68. I. Hamada, Y. Morikawa, Density-Functional Analysis of Hydrogen on Pt(111): Electric Field, Solvent, and Coverage Effects, J. Phys. Chem. C. 112 (2008) 10889–10898.
69. Q. Shi, R. Sun, Adsorption manners of hydrogen on Pt(1 0 0), (1 1 0) and (1 1 1) surfaces at high coverage, Comput. Theor. Chem. 1106 (2017) 43–49.
70. L. Yan, Y. Sun, Y. Yamamoto, S. Kasamatsu, I. Hamada, O. Sugino, Hydrogen adsorption on Pt(111) revisited from random phase approximation, J. Chem. Phys. 149 (2018) 164702.
71. C. Jimenez-Orozco, E. Florez, F. Vines, J.A. Rodriguez, F. Illas, Critical hydrogen coverage effect on the hydrogenation of ethylene catalyzed by δ-MoC(001): an ab initio thermodynamic and kinetic study, ACS Catalysis, 10 (2020) 6213–6222.